APEM journal
Advances in Production Engineering & Management **ISSN 1854-6250**
Volume 19 | Number 3 | September 2024 | pp 386–394 Journal home: apem-journal.org
https://doi.org/10.14743/apem2024.3.514 Original scientific paper

Enhancing calibration accuracy with laser interferometry for high-resolution measuring systems

Lipus, L.C.[a], Acko, B.[a,*], Klobucar, R.[a]

[a]University of Maribor, Faculty of Mechanical Engineering, Slovenia

A B S T R A C T

This paper presents an analysis of the measurement capability of laser interferometry for calibrating high-resolution measuring systems, focusing on potential errors that need to be carefully controlled to ensure adequate metrological traceability. The primary scientific research focus of our National Dimensional Metrology Laboratory is the development of metrological applications for industry, with ongoing improvements in calibration procedures for measuring machines and tools. Through a review of possible error sources, an innovative approach to reducing the most significant factors is proposed. This is specifically applied to the following calibration cases: field calibration of coordinate measuring machines, and laboratory calibration of precision probes and line scales. Instrumental and environmental errors can be effectively mitigated by using periodically calibrated laser interferometers in well-controlled air conditions, ensuring an uncertainty of 0.2 µm/m. Most geometrical errors can be minimized by precise adjustments to the interferometry and positioning systems, achieving an uncertainty of 0.3 µm/m. However, errors caused by temperature differences in the material along the measuring path remain the most influential. These arise due to the high expansion coefficient of the material and some uncertainty in its properties. After several hours of temperature stabilization, using three temperature sensors along the displacement range for software compensation, temperature differences still contribute significantly to measurement uncertainty. For example, the error is 0.5 µm/min in the case of line scale calibration and 1.1 µm/m for coordinate measuring machine calibration.

A R T I C L E I N F O

Keywords:
Laser interferometry;
High resolution measurements;
Measurement uncertainty;
Dimensional metrology;
Coordinate measuring machine;
Precise probe;
Line scale

**Corresponding author:*
bojan.acko@um.si
(Acko, B.)

Article history:
Received 24 July 2024
Revised 26 October 2024
Accepted 28 October 2024

1. Introduction

A wide range of verification methods, based on various measurement standards, is used for calibrating and determining geometric errors in high-resolution measuring systems. Among these, laser-based methods are the most accurate. Precision measuring machines used in industry typically have an uncertainty of around µm per meter in the measuring range. Sub-micrometer accurate measures, such as gauge blocks, setting rings, cylinders, step gauges, and line scales, are commonly employed to ensure their measurement traceability. Displacement lasers, known for their exceptional accuracy, often exceed manufacturing tolerance requirements. They are used in situations where more precise and detailed information about the properties of a metrological system is needed, such as in advanced monitoring of workpiece geometry in the automotive industry [1-3].

Our National Dimensional Metrology Laboratory is constantly improving the capability of our calibration and measurement procedures. The core of our research is characterization of current laboratory equipment to minimize errors, and development of new measurement procedures for calibrating highly precise instruments and machines. Primary task in the field of scientific and Industry metrology of the laboratory is maintaining the national standard for length and assuring measurements traceability in Slovenian industry. For this purpose, the laboratory is accredited for length-calibrations of standards and measuring equipment by Slovenian Accreditation (SA). Its metrology capabilities are published in the database of national metrology institutes at the International Bureau of Weights and Measures (KCDB BIPM). The main focus of scientific research work of the laboratory is development of metrological applications for practical use in industry, science and other branches. We are also performing activities for customers in the field of industry and science metrology, as well as education for calibrations.

To ensure measurement traceability, all potential error sources must be analyzed to identify and reduce the most influential factors in real-world environmental conditions, thereby achieving proper measurement accuracy. In a laser interferometric system, laser interferometers and corresponding air sensors should be periodically calibrated, while the entire instrumental system can be directly checked through comparison measurements with a reference laser interferometer [4]. This paper presents several metrological laser interferometry (LI) systems with innovative adjustments for error mitigation, developed in our laboratory, and summarizes the uncertainty budget, which is generally applicable to other similar high-precision metrological systems.

2. Measurement system and adjustments

Measurement systems with laser interferometer (LI) provide very precise position or distance information. It consists of a laser head, which produces the beam of highly stabilized, low-power light, and a variety of optical components and accessories such as air and material sensors. Laser interferometry is based on the principle of Michelson interferometer: a beam splitter divides the light beam into two beams, the reference beam is returned by a fixed reflector and another one returns from the retroreflector which is shifted along the measured path. Combined by the splitter, they interfere into pulses, which are counted by a photo-electro detector inside the laser head (Fig. 1).

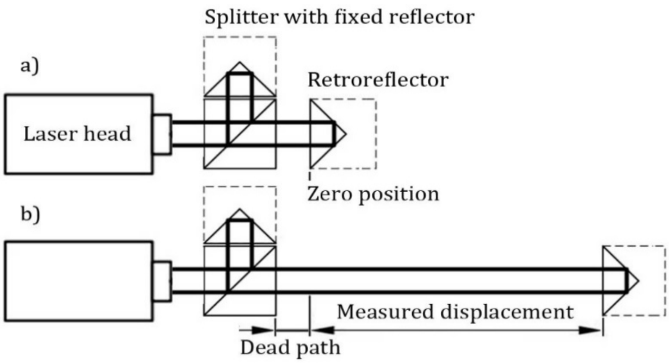

Fig. 1 The principle of Michelson interferometer

A calibration procedure generally comprehends the following basic steps:

- Installation and precise alignment of laser head and optics. Special mounting elements are constructed for the optics used for specific calibrations.
- The air conditions shall be stabilized for at least 5 hours. Three material temperature sensors are usual used for material and one air sensor to observe temperature, pressure and humidity along the measuring path.
- Deviations are then measured in eleven points (zero point and ten equal increments along the whole measuring length, or more by a customer's request), repeated three times in each point.

Generally, there are three categories of potential measurement errors: geometrical, environmental, and instrumental. The methods upgraded in our laboratory to mitigate these errors are presented in the following subsections.

2.1 Geometrical errors

The most of geometrical errors can be eliminated by applying a precise alignment procedure. The cosine error occurs when the beam from laser and the axis of the stage motion are not completely parallel (Eq. 1), while Abbe error occurs due to sloping of the retroreflector. Firstly, the beam is aligned by parallel shifts of the laser head into the centre of the target at close position, then by angle adjustments at maximum displacement.

$$e_{\cos} = L(\cos\varphi - 1) \approx -L\varphi^2/2 \tag{1}$$

where φ is angle between the beam and the axis of the moving stage, and L is the displacement.

When calibrating one-coordinate measuring machines (CCMs) of various types, the retroreflector is attached to the moving probe (Fig. 2), and the cosine error is eliminated by aligning the system at the maximum possible displacement. The LI system is used for calibration of CCMs with measuring length minimal 1 m, while CCMs with shorter measuring length are calibrated with gauge blocks. Assuming an adjustment at a minimum length of 1 m and visual centering of the beam within ± 1 mm, the maximum cosine error, as calculated by Eq. 1, is $0.5 \times 10^{-6} \times L$. The uncertainty is calculated by reduction with $\sqrt{3}$ at assumption of rectangular distribution, $u_{\cos} \approx 0.3 \times 10^{-6} \times L$.

Abbe error can be minimized within the resolution of CMM, which is minimally ± 5 nm for the best machine with digital display. The position of the optical elements and the moving parts are set in such way, that the measured object axis is set in the line with the center of the laser linear retroreflector. It allows the Abbe errors to be reduced to negligible levels even for the most demanding dimensional metrology tasks [5, 6]. Generally, for a maximal error 15 nm, the Abbe uncertainty is $u_{\mathrm{a}} = 0.009$ nm. The best mitigation of the Abbe error can reduce it to just a few nanometers.

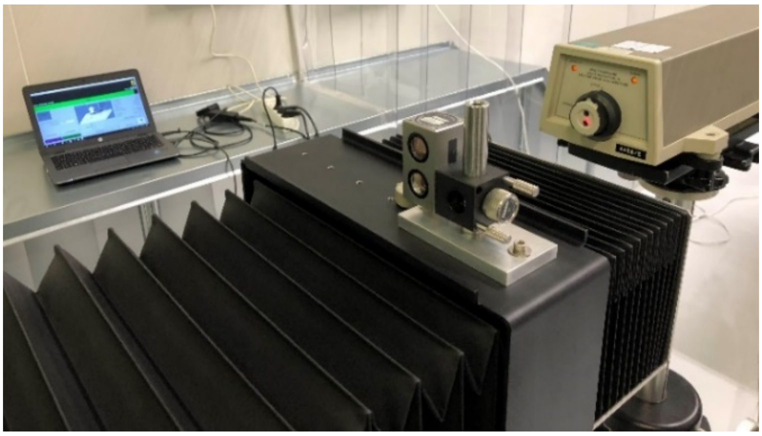

Fig. 2 Set-up for calibration of a one-coordinate measuring machine

When calibrating a precise probe, the retroreflector is installed below the probe (Fig. 3). The ceramic gauge is used as a base, and its surface imperfections are eliminated by setting the zero position. Precise probe is fixed, while the shift along its measurement range is performed by horizontal shifting the base with moving table, which has angle variation up to 15 micro-radians. When visual centering the probe onto retroreflector with offset ± 1 mm, the Abbe error is maximally ± 15 nm. The cosine error of the probe is eliminated by using dial indicator (Fig. 4). Within deviations ± 2 µm along the optic's frame 40 mm, the cosine error is negligible, $1.25 \times 10^{-9} \times L$, where L is probe's measurement range, commonly with resolution ± 5 nm. When calibrating the one-coordinate measuring machine, the cosine error of the laser head is adjusted horizontally along the moving table. By visual centering ± 1 mm at minimal distance 1 m, the maximal cosine error is achieved $0.5 \times 10^{-6}\, L$, and the uncertainty $u_{\cos} \approx 0.3 \times 10^{-6} \times L$.

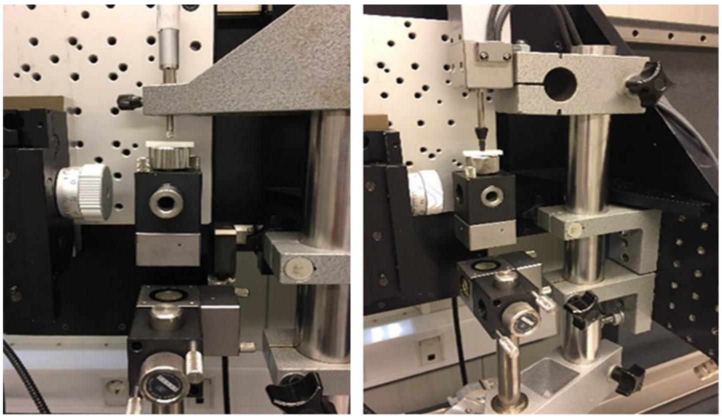

Fig. 3 Set-up for calibration of precise probe

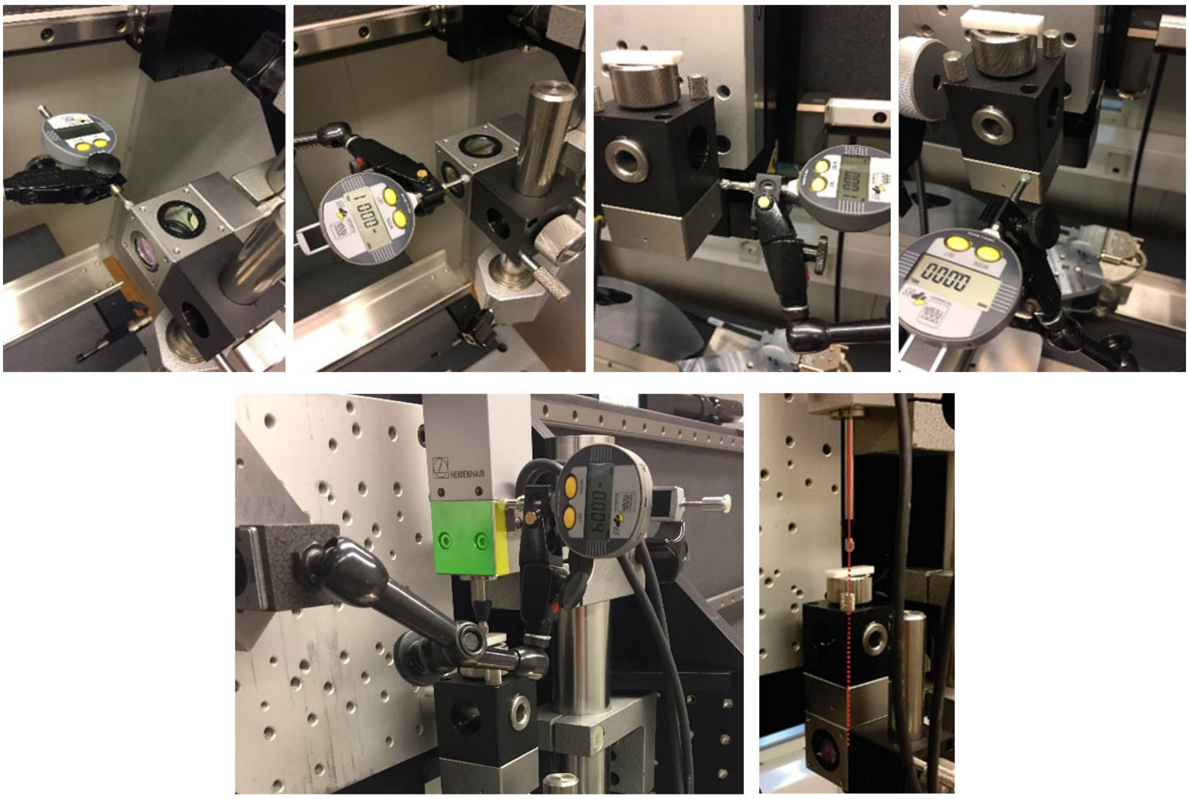

Fig. 4 Pitch and yaw measurements of the stage in y-direction

When calibrating a line scale, it is shifted using a movable table, and the centers of the line marks are precisely located by a video system with a high-resolution camera and software designed to detect the center of dark regions. A laser interferometer is then used to measure displacement from the zero position of the line scale, with a retroreflector fixed onto the moving table (Fig. 5). Similarly to the previous case, the beam is aligned along the moving table at maximal displacement and the camera's axis is adjusted by using dial indicator. The geometrical error of the moving table in the x- and z-directions (within the coordinate system that includes the optics, camera, and line scale, as shown in Fig. 6) was determined empirically [2]. For pitch, the largest angle difference along the 500 mm measurement path was 7 µm/m. The maximum offset of the laser retroreflector in the z-direction was estimated to be 3 mm, resulting in an expected error interval for pitch of 7 nm/mm × 3 mm = 21 nm. For yaw, the largest angle difference along the 500 mm measurement path was 10 µm/m. The maximum offset of the laser retroreflector in the x-direction was estimated to be 1 mm, resulting in an expected error interval for yaw of 10 nm/mm × 1 mm = 10 nm. Total error of table inclination, calculated by Pythagorean Theorem, is 23 nm, so the Abbe uncertainty is maximally $u_{\mathrm{a}} = 0.013$ nm.

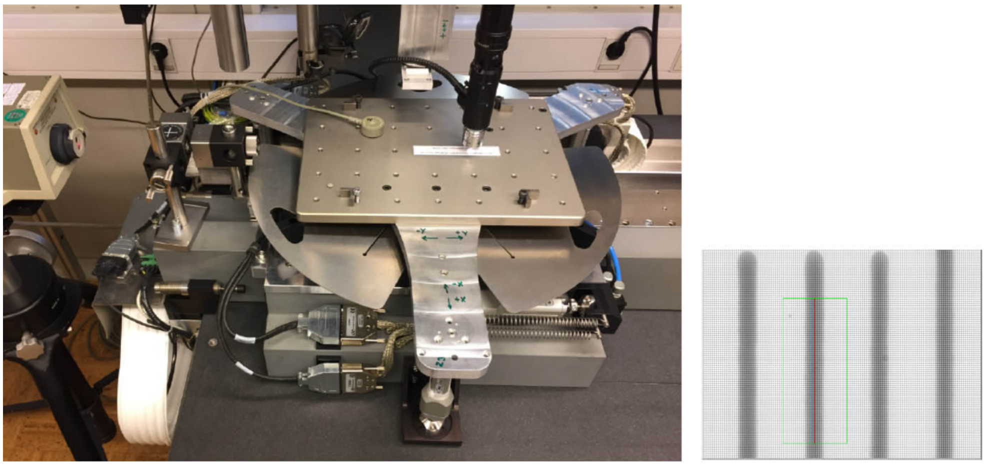

Fig. 5 Set-up for calibration of line scale with video detecting of line-mark position

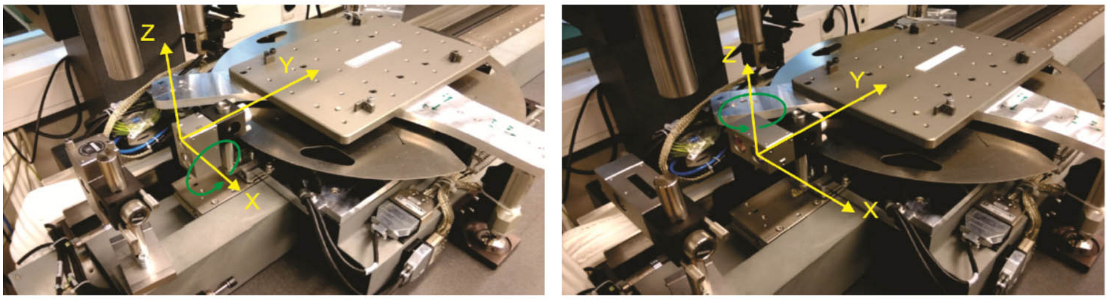

Fig. 6 Alignment of optics, camera and the moving table with fixed line scale

2.2 Environmental errors

Environmental errors occur due to thermal properties of the machine under test and due to dependence of the light wavelength on the atmospheric conditions. Usually, three material temperature sensors are used along the measuring path, and one air sensor for measuring temperature, pressure and humidity. High-quality laser interferometers maintain a stable and repeatable light frequency, which is negligible compared to the uncertainty of the sensors. The LI software automatically compensates the material path length with the material sensors and the vacuum wavelength with air refractive index, which depends on the pressure p, temperature T and humidity H, and was empirically determined by Edlen's equation (with coefficients -0.955×10^{-6} / K, 0.268×10^{-6} / hPa and -0.0085×10^{-6} / % of air humidity).

The compensation uncertainty depends on variation of air parameters along the measuring path and sensors' sensitivity. The sensitivity of common high-quality air sensors is around $0.15 \times 10^{-6} \times L$, including possible drift through years of application [3]. At common variations of air parameters in well-controlled conditions during field calibrations (0.5 K, 0.5 hPa, and 10 % humidity fluctuation) along the measuring path, and applying Edlen's coefficients along with a reduction by the square root of three for an assumed rectangular distribution [7], the total uncertainty for air compensation is $0.3 \times 10^{-6} \times L$. In well controlled conditions in laboratory chamber, where air temperature 20 °C varies just ± 0.1 K, the total uncertainty for air compensation is $0.2 \times 10^{-6} \times L$.

Dead path error is caused by an uncompensated length of the laser beam between the interferometer and the retroreflector, with the machine stage at zero position (Fig. 1). It gets negligible by placing the linear interferometer optics close to the zero point of the moveable retroreflector. At $L = 10$ mm in well controlled conditions, we get maximally 3 nm, which is practically negligible in comparison to the best resolution of the calibrated devices, described here. Also, the counting system of modern laser interferometers have negligible influence. Both contributes a variation of the displayed result L_{LI} on level of nm, usually eliminated by choosing LI resolution of 0.01 µm. So, the maximal permissible uncertainty of the indication of the laser interferometer, including air compensation, stability of light stability, counting system and dead path, is taken:

$$u_{\mathrm{LI}} = 10\ \mathrm{nm} + 0.3 \times 10^{-6} \times L \quad \text{at field conditions} \tag{2a}$$

$$u_{\mathrm{LI}} = 10\ \mathrm{nm} + 0.2 \times 10^{-6} \times L \quad \text{at conditions in chamber} \tag{2b}$$

where nominal length L is expressed in metres.

The software correction uncertainty strongly depends on the uncertainty of thermal expansion coefficient, α. For coordinate measuring machines, we take $\alpha = (11 \pm 1) \times 10^{-6}$/K, and for precise probes we take $\alpha = (8 \pm 1) \times 10^{-6}$/K. While in case of line scales made of glass, steel or other material, having quite different temperature expansion coefficients, in many cases not exactly known, we take $\alpha = (10 \pm 2) \times 10^{-6}$/K. Assuming rectangular distribution, their uncertainty u_α is calculated from deviations by reducing with $\sqrt{3}$. To provide minimal temperature deviations along the measuring path, calibrations are performed after temperature stabilization of the measuring machines, e.g. at least of 5 hours stabilization at field calibrations, and at least of 24 hour stabilization in the chamber. Temperature of the calibrated device is measured with three material temperature sensors, installed along the measuring path.

For our case of material temperature sensors, the uncertainty is maximally 0.015 K, evaluated from their calibration certificates (including expanded calibration uncertainty 0.015 K, reduced by 2, and maximal deviation 0.016 K and long term maximal drift 0.016 K, both reduced by $\sqrt{3}$).The temperature deviation of the device (from standard temperature 20 °C) is calculated as a mean value θ of the three measured deviations. Assuming maximal variation ± 0.3 K in field well controlled conditions, the uncertainty of the mean temperature is $0.3\ \mathrm{K}/\sqrt{3{\times}3} = 0.1$ K. The total standard uncertainty is less than $u_\theta = \sqrt{0.015^2 + 0.1^2}\ \mathrm{K} = 0.1$ K, while for cases in the chamber with maximal temperature variation ± 0.1 K, we get $u_\theta = \sqrt{0.015^2 + 0.033^2}\ \mathrm{K} = 0.04$ K and take 0.05 K into calculation of total calibration uncertainty.

3. Results and discussion

The measurement accuracy of the specific calibration process is calculated from following mathematical model of the measured deviation:

$$e = L_{\mathrm{i}} \cdot (1 + \alpha \cdot \theta) - (L_{\mathrm{LI}} - e_{\mathrm{g}}) \tag{3}$$

where parameters are:

- L_{i} indicated value on the calibrated device
- α thermal expansion coefficient of the measurement system of the device at 20 °C
- θ temperature deviation of the measurement system of the device from 20 °C
- L_{LI} length indicated by the laser interferometer
- e_{g} geometrical error of the measurement system

Combined standard uncertainty is calculated according to GUM [7] by the equation:

$$u_{\mathrm{e}}^2 = (c_{\mathrm{i}} \cdot u_{\mathrm{i}})^2 + (c_\alpha \cdot u_\alpha)^2 + (c_\theta \cdot u_\theta)^2 + (c_{\mathrm{LI}} \cdot u_{\mathrm{LI}})^2 + (c_{\mathrm{g}} \cdot u_{\mathrm{g}})^2 \tag{4}$$

where coefficients are partial derivatives of the expression (3):

$c_{\mathrm{i}} = \partial e/\partial L_{\mathrm{i}} = 1 + \alpha_{\mathrm{m}} \cdot \theta_{\mathrm{m}} \approx 1$ at well controlled temperature conditions
$c_\alpha = \partial e/\partial \alpha_{\mathrm{m}} = \theta \cdot L_{\mathrm{i}} \approx \theta \cdot L$, where L is measured length
$c_\theta = \partial e/\partial \theta_{\mathrm{m}} = \alpha \cdot \mathrm{L_i} \approx \alpha \cdot L$
$c_{\mathrm{LI}} = \partial e/\partial L_{\mathrm{LI}} = -1$
$c_{\mathrm{g}} = \partial e/\partial e_{\mathrm{g}} = 1$

and partial uncertainties are evaluated from errors, discussed before. Resolution, repeatability, and actual temperature deviation of the calibrated instrument are considered.

For the best-known one-dimensional measuring device with digital reading, 10 nm resolution and 0 nm repeatability, the reading error is within ± 0.005 μm. At assumed rectangular distribution, the indication uncertainty is $u_{\mathrm{i}} = 0.005\ \mu\mathrm{m}/\sqrt{3} = 0.003\ \mu\mathrm{m}$. At calibration of line scales using high-resolution video system (Table 3), the indication uncertainty is $u_{\mathrm{i}} = 0.025$ μm.

The combined standard uncertainty calculated by Eq. 3 is given in tables 1-3 for three different calibrations, for best presumed devices and conditions. The expanded uncertainty by Eqs. 5 is double value of the standard uncertainty, covering 95 % possibility of the measurement results. The first term in Eq. 5a is negligible yielding linear graph (Fig. 7a), while the sub-micrometre graphs (Figs. 7b and 7c) have comparable terms, with equal value at 30 mm in Eq. 5b and at 50 mm in Eq. 5c.

Tables 1-3 present the basic contributions of measurement uncertainty in length calibration procedures using the laser interferometry. With the presented measurement uncertainty, we can ensure traceability to calibration laboratories and industry. In the following, the methods and possible improvements to reduce the measurement uncertainty will be described.

For reducing the measurement uncertainty, we must always analyse and find the maximal contributions in the uncertainty budget. In Tables 1-3, where the measurement uncertainty budget is covered, the laser interferometry, the environmental temperature and the cosine error have the greatest influence on the measurement uncertainty. The impact of laser interferometry could be improved with better environmental sensors. Researchers [8] propose to measure the distance with laser interferometry in a vacuum, but such an approach is very expensive and impractical to implement. The uncertainty of the linear temperature coefficient could be reduced by an accurate knowledge of the material, but this determination is very critical in the length measurements. In the procedures described above, environmental temperature and cosine error for positioning the laser beam stand out the most. Minimizing the temperature effect could be eliminated with better environmental conditions, but it is very difficult to achieve environmental temperature deviation below 0.1 K. Temperatures could be measured in several points and perform real-time temperature compensation, as suggested by certain authors [1]. Even such a temperature measurement system is expensive and requires good handling and detailed analysis. Minimizing the cosine error could be eliminated with a better positioning system [3]. The authors presented a digital system for laser beam positioning. Such a system is sensitive to outside light and needs to be controlled. Proposed methods can contribute to more accurate measurement capabilities. However, they require additional investment and knowledge.

Table 1 Uncertainty budget for calibration of one coordinate measuring devices

Variable	Standard uncertainty	Distribution	Sensitivity coefficient	Uncertainty contribution
L_i	0.003 µm	Rectangular	1	0.003 µm
α	0.58×10^{-6} K^{-1}	Rectangular	0.2 K $\times L$	$0.12 \times 10^{-6} \times L$
θ	0.1 K	Normal	11×10^{-6}K$^{-1} \times L$	$1.1 \times 10^{-6} \times L$
L_{LI}	0.01 µm + $0.3 \times 10^{-6} \times L$	Normal	-1	0.01 µm + $0.3 \times 10^{-6} \times L$
e_{cos}	$0.3 \times 10^{-6} \times L$	Rectangular	1	$0.3 \times 10^{-6} \times L$
e_a	0.009 nm	Rectangular	1	0.009 nm
			Total:	$\sqrt{(0.014\ \mu\text{m})^2 + (1.19 \times 10^{-6} \times L)^2}$

The expanded uncertainty for calibration of one coordinate measuring devices is:

$$U = \sqrt{(0.03\ \mu\text{m})^2 + (2.4 \times 10^{-6} \times L)^2} \tag{5a}$$

Table 2 Uncertainty budget for calibration of precise probes

Variable	Standard uncertainty	Distribution	Sensitivity coefficient	Uncertainty contribution
L_i	0.003 µm	Rectangular	1	0.003 µm
α	0.58×10^{-6} K^{-1}	Rectangular	0.1 K $\times L$	$0.06 \times 10^{-6} \times L$
θ	0.05 K	Normal	8×10^{-6}K$^{-1} \times L$	$0.4 \times 10^{-6} \times L$
L_{LI}	0.01 µm + $0.2 \times 10^{-6} \times L$	Normal	-1	0.01 µm + $0.2 \times 10^{-6} \times L$
e_{cos}	$0.3 \times 10^{-6} \times L$	Rectangular	1	$0.3 \times 10^{-6} \times L$
e_a	0.009 nm	Rectangular	1	0.009 nm
			Total:	$\sqrt{(0.014\ \mu\text{m})^2 + (0.54 \times 10^{-6} \times L)^2}$

The expanded uncertainty for calibration of precise probes is:

$$U = \sqrt{(0.03\ \mu\text{m})^2 + (1.1 \times 10^{-6} \times L)^2} \tag{5b}$$

Table 3 Uncertainty budget for calibration of line scales

Variable	Standard uncertainty	Distribution	Sensitivity coefficient	Uncertainty contribution
L_i	0.025 µm	Normal	1	0.025 µm
α	1.155×10^{-6} K^{-1}	Rectangular	$0.1\ \mathrm{K} \times L$	$0.1 \times 10^{-6} \times L$
θ	0.05 K	Normal	$10 \times 10^{-6}\ \mathrm{K}^{-1} \times L$	$0.5 \times 10^{-6} \times L$
L_{LI}	$0.01\ \mu\mathrm{m} + 0.2 \times 10^{-6} \times L$	Normal	-1	$0.01\ \mu\mathrm{m} + 0.2 \times 10^{-6} \times L$
e_{cos}	$0.3 \times 10^{-6} \times L$	Rectangular	1	$0.3 \times 10^{-6} \times L$
e_a	0.013 nm	Rectangular	1	0.013 nm
			Total:	$\sqrt{(0.03\ \mu\mathrm{m})^2 + (0.63 \times 10^{-6} \times L)^2}$

The expanded uncertainty for calibration of line scales is:

$$U = \sqrt{(0.06\ \mu\mathrm{m})^2 + (1.25 \times 10^{-6} \times L)^2} \tag{5c}$$

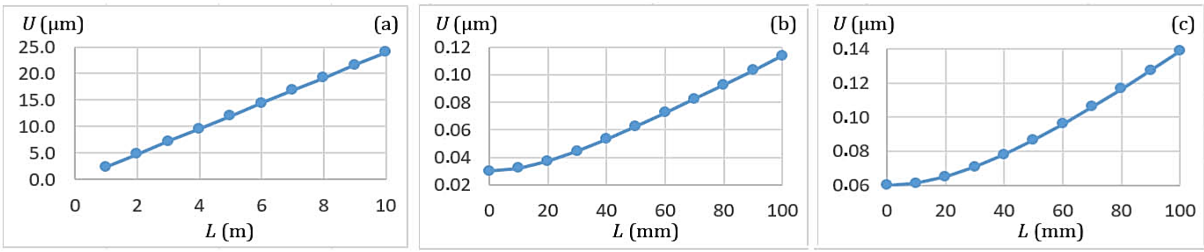

Fig. 7 Expanded calibration uncertainty: (a) one-dimensional coordinate measuring devices, (b) precise probes, (c) line scales

When measuring samples, the first term rises due to surface error, depending on sample's quality. While roughness of fine polished gauge blocks varies 15-30 nm [9, 10], geometrical imperfections have a sub-micrometre contribution [11]. Incrementally formed samples had roughness 0.4-0.75 µm [12], cylinders after turning had waviness 25-100 nm [13], and roughness after polishing 25-50 nm [14]. The waviness of a setting ring (Fig. 8) in contact with probes contributes 25-50 nm.

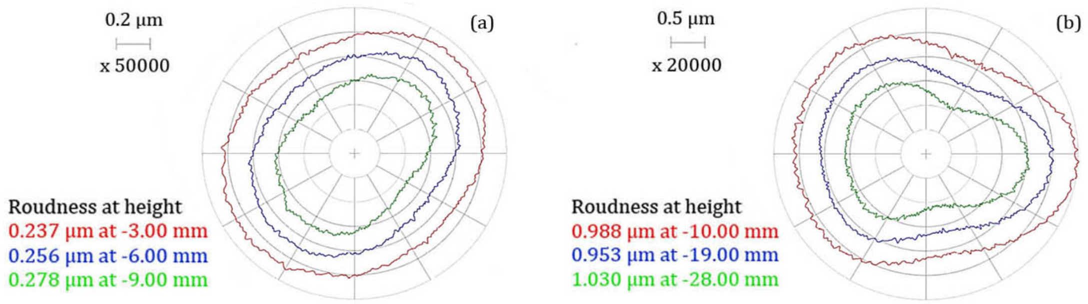

Fig. 8 Roundness profile of setting rings with diameter: (a) 50 mm, (b) 150 mm

4. Conclusion

Proper procedures with calibrated standards, deployable on machine tools, and effective error mitigation in real-world environmental conditions are essential to ensure the required measurement accuracy. Calibration procedures typically offer seven to ten times better accuracy than the calibrated device, ensuring proper metrological traceability. The uncertainty budget was presented for three specific cases of improved setups, chosen among the procedures used in our laboratory and verified by the national accreditation body. For highly precise calibration, our laboratory developed specific positioning systems applying a precise moving table, upgraded with clamping system and video probe system, adjusted with dial gauges, as detailed in the paper. By reviewing potential error sources in the measuring system, we found that using high-quality, periodically calibrated laser interferometers and sensors in well-controlled air conditions effectively mitigates instrumental and environmental errors. Geometrical errors can also be significantly reduced through precise adjustments of optics and probes. The majority of errors in the uncertainty budget are proportional to the displacement length, with the absolute term only becoming noticeable at shorter displacements (up to 100 mm). When calibrating gauge samples, such as cylinders and rings, the surface error contributes essentially, while Abbe and dead-path errors in the absolute term become negligible. The most significant errors arise from material temperature differences along the measuring path. After several hours of stabilization and using three material temperature sensors along the path, this error remains the primary contributor. When further mitigation is necessary, such as for the calibration of step gauges, a more advanced monitoring system for material temperature was developed in our laboratory. Based on the content and measurement uncertainty calculations presented in the article, we provide the current needs of industry and calibration laboratories. Improvements and future work are also proposed. These enhancements could reduce measurement uncertainties but would require additional investments and expertise for implementation.

Acknowledgement

The authors acknowledge the financial support from the Slovenian Research Agency (Research Core Funding No. P2-0190, Grant numbers 1000-20-0552, 6316-3/2018-255, 603-1/2018-16), as well as from the Metrology Institute of the Republic of Slovenia (funding of national standard of length; Contract No. C3212-10-000072). Furthermore, the authors would like to acknowledge the use of research equipment for processing and monitoring the machining and forming processes: Laser measuring systems for machine tools and coordinate measuring machines, procured within the project "Upgrading national research infrastructures – RIUM", which was co-financed by the Republic of Slovenia, the Ministry of Education, Science and Sport and the European Union from the European Regional Development Fund.

References

[1] Šafarič, J., Dolšak, B., Klobučar, R., Ačko, B. (2020). Analysis of thermal contribution to the measurement uncertainty in step gauge calibration, *Precision Engineering,* Vol. 66, No. 52-61, doi: 10.1016/j.precisioneng.2020.06.012.

[2] Klobucar, R., Acko, B. (2017). Automatic high resolution measurement set-up for calibrating precise line scales, *Advances in Production Engineering & Management*, Vol. 12, No. 1, 88-96, doi: 10.14743/apem2017.1.242.

[3] Safaric, J., Klobucar, R., Acko, B. (2021). Measurement setup and procedure for precise step gauge calibration, *IEEE Transactions on Instrumentation and Measurement*, Vol. 70, Article No. 1009610, doi: 10.1109/TIM.2021.3115579.

[4] Lipus, L.C., Budzyn, G., Acko, B. (2021). Analysis of laser interferometer measurement uncertainty by simulating error sources, *International Journal of Simulation Modelling,* Vol. 20, No. 2, 339-350, doi: 10.2507/IJSIMM20-2-563.

[5] Köning, R., Weichert, C., Köchert, P., Guan, J., Flügge, J. (2013). Redetermination of the abbe errors' uncertainty contributions at the nanometer comparator, In: *Proceedings of the 9th International Conference on Measurement,* Smolenice, Slovakia, 171-174.

[6] Leach, R. (2014). Abbe error/offset, In: Laperrière, L., Reinhart, G. (eds.), *CIRP Encyclopaedia of production engineering*, Springer, Berlin, Germany, 1-4, doi: 10.1007/978-3-642-35950-7_16793-1.

[7] Guide to the expression of uncertainty in measurement GUM 1995, from *https://www.bipm.org/utils/common/documents/jcgm/JCGM_100_2008_E.pdf*, accessed September 14, 2024.

[8] Flügge, J., Weichert, C., Hu, H., Köning, R., Bosse, H., Wiegmann, A., Schulz, M., Elster, C., Geckeler, R.D. (2009). Interferometry at the PTB nanometer comparator: Design, status and development, In: *Proceedings of SPIE 7133, Fifth International Symposium on Instrumentation Science and Technology,* Shenyang, China, Article No. 713346, doi: 10.1117/12.821252.

[9] Buchta, Z., Šarbort, M., Čížek, M., Hucl, V., Řeřucha, Š., Pikálek, Z., Dvořáčková, Š., Dvořáček, F., Kůr, J., Konečný, P., Weigl, M., Lazar, J., Číp, O. (2017). System for automatic gauge block length measurement optimized for secondary length metrology, *Precision Engineering*, Vol. 49, 322-331, doi: 10.1016/j.precisioneng.2017.03.002.

[10] Ali, S.H.R., Naeim, I.H. (2014). Surface imperfection and wringing thickness in uncertainty estimation of end standards calibration, *Optics and Lasers in Engineering* Vol. 60, 25-31, doi: 10.1016/j.optlaseng.2014.03.012.

[11] Lipus, L.C., Acko, B., Tompa, J. (2022). Experimental determination of influences on a gauge block's stack length, *Advances in Production Engineering & Management*, Vol. 17, No. 3, 339-349, doi: 10.14743/apem2022.3.440.

[12] Visagan, A., Ganesh, P. (2022). Parametric optimization of two point incremental forming using GRA and TOPSIS, *International Journal of Simulation Modelling*, Vol. 21, No. 4, 615-626, doi: 10.2507/IJSIMM21-4-622.

[13] Tomov, M., Gecevska, V., Vasileska, E. (2022). Modelling of multiple surface roughness parameters during hard turning: A comparative study between the kinematical-geometrical copying approach and the design of experiments method (DOE), *Advances in Production Engineering & Management*, Vol. 17, No. 1, 75-88, doi: 10.14743/apem2022.1.422.

[14] Yao, W., Lyu, B., Zhang, T., Guo, L., Song, Y. (2023). Effect of elastohydrodynamic characteristics on surface roughness in cylindrical shear thickening polishing process, *Wear*, Vol. 530-531, Article No. 205026, doi: 10.1016/j.wear.2023.205026.